

## Field-squeeze operators via coherent population trapping

Qingping Hu,<sup>1,2</sup> Xiangming Hu,<sup>1,\*</sup> Liang Hu,<sup>1</sup> and Guanghui Wang<sup>1</sup>

<sup>1</sup>College of Physical Science and Technology, Central China Normal University, Wuhan 430079, People's Republic of China

<sup>2</sup>Institute of Technical Physics, SEEE, Wuhan Textile University, Wuhan 430073, People's Republic of China



(Received 25 September 2018; published 2 January 2019)

We present a scheme to generate unitarily two-mode and four-mode field squeezing in optical cavities with the near-resonantly dressed three-level atoms in the  $\Lambda$  configuration. The dressing fields open two coherent population trapping (CPT) windows, within which the atoms stay predominantly in the dark state and yield strong nonlinearities for both the dressing fields themselves and the other applied fields. The two-mode squeeze operator is separated from degrees of freedom of atoms in a common CPT window, and the multimode squeeze operator is segregated in different CPT windows. The resulting two-mode and multimode interaction strengths are at least one order higher than in the previous dispersive schemes, where all fields are far off resonant with the atoms. The present near-resonant scheme is robust to spontaneous emission since atoms are nearly trapped in a long-lived superposition state.

DOI: [10.1103/PhysRevA.99.013805](https://doi.org/10.1103/PhysRevA.99.013805)

### I. INTRODUCTION

Squeezing is one of the key concepts in quantum optics and laser physics because of its fundamental importance and its wide applications in high-precision measurements and quantum communications. Squeezed states have less quantum fluctuations in one quadrature than a coherent state has [1–3]. Of particularly important interest is the two-mode squeezing, which is closely correlated with continuous variable entanglement. Moreover, when the squeezing parameter is large one can have Einstein-Podolsky-Rosen (EPR) entanglement [4,5].

In the usual cases [1–3], on resonance or close to resonance, atoms are excited and their spontaneous emission destroys any possible squeezing of the coupled optical fields. In order to overcome the spontaneous emission and to seek for squeezing, one has to work in the far-off-resonance regimes, where  $\Omega_l/|\Delta_l| \ll 1$  ( $\Omega_l$  are real Rabi frequencies associated with the  $l$ th driving fields and  $\Delta_l$  are the detunings of the atomic frequencies from the driving field frequencies). In the far-off-resonance regimes, the atoms are hardly excited and then there is hardly spontaneous emission [3]. At the same time, the dispersive interactions are dominant over the absorptive interactions. There have been existing schemes that are based on this and separate out the field-squeeze operator from the coupled atoms [6–9]. Reid *et al.* [6] early introduced the phenomenological Hamiltonian of the parametric form  $\hbar(\xi^* a_1 a_2 + \xi a_1^\dagger a_2^\dagger)$  from the far-off-resonant three-level atoms in  $\Lambda$  configuration, where  $a_{1,2}$  and  $a_{1,2}^\dagger$  are the annihilation and creation operators. Guzmán *et al.* [7] presented an explicit analysis on the method of producing single- and two-mode squeeze operators. This method was also applied to multimode cases and to the other level schemes [8,9]. In these schemes the far-detuned driving fields contribute to the cavity

mode parametric down-conversion strengths only the second-order small quantities  $O(\Omega_k/\Delta_k)O(\Omega_l/\Delta_l)$ . This means that we are faced with a challenge to increase the parametric interaction strengths. Once they are too much smaller than the cavity damping rates, squeezing can no longer appear in the output fields.

Now the natural question we are faced with is, can we isolate the field-squeeze operators from the degrees of freedom of the near-resonantly driven atoms ( $|\Delta_l|/\Omega_l \ll 1$ )? The answer is yes. Our scheme is based on coherent population trapping (CPT) [10], which is one of the most remarkable coherence effects in light-matter interactions. When two optical fields interact resonantly with three-level  $\Lambda$  atoms [as shown in Fig. 1(a)], the atoms are pumped into a superposition of the ground states and are no longer excited. This coherent phenomenon is based on “dark resonance” [10–14]. The superposition state in which the atoms are populated is called the “dark state.” Once the atoms enter the dark state, they are no longer excited and so become transparent to the applied fields [Fig. 1(b)]. It is the dark resonance that underlies those well-known coherent effects such as CPT and electromagnetically induced transparency [11–14]. One of the greatest interests is in giant nonlinearities close to the dark resonance. The ratio of dispersion to absorption will be much larger than that under other circumstances when the system approaches resonance [Fig. 1(c)]. Another important point is that all population is almost trapped in the dark state, and spontaneous emission is hardly involved in the quantum noise manipulation. As will be shown below, the above two advantages of the CPT system are perhaps the best conditions for the creation of squeezed states.

In this paper we show that the unitary field-squeeze operators can be isolated from the degrees of the nearly resonant atoms. CPT happens when the dressing fields are on two-photon resonances with the three-level atoms on the  $\Lambda$  dipole-allowed transitions. When we tune the dressing fields, there exist two frequency windows, which center at the atomic resonance frequencies and within which CPT occurs

\*Corresponding author: [xmhu@mail.ccnu.edu.cn](mailto:xmhu@mail.ccnu.edu.cn)

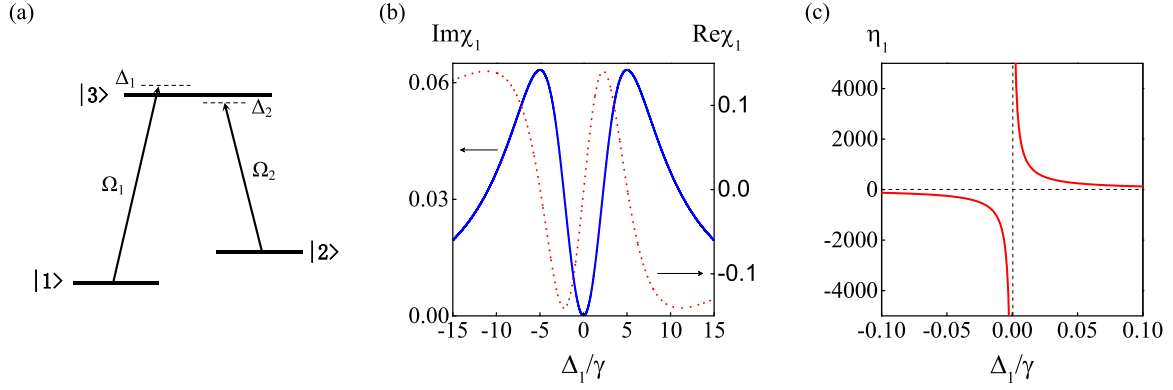


FIG. 1. (a) Interaction of three-level atom with two dressing fields in  $\Lambda$  configuration with Rabi frequencies  $\Omega_{1,2}$  and detunings  $\Delta_{1,2}$ . (b) The absorption  $\text{Im}\chi_1$  (real line) and dispersion  $\text{Re}\chi_1$  (dashed line) in units of  $|\mu_{13}|^2/(\epsilon_0\hbar)$  versus the normalized detuning  $\Delta_1/\gamma$  ( $\Delta_2 = -\Delta_1$ ) for given Rabi frequencies  $\Omega_{1,2} = 5\gamma$  ( $\gamma_{1,2} = \gamma$ ). The deep dip of the symmetric solid curve opens a window for CPT at  $\omega_{31}$  (i.e.,  $\Delta_1 = 0$ ). (c) The ratio of the dispersion to the absorption  $\eta_1 = \text{Re}\chi_1/\text{Im}\chi_1$  shows a giant value in the central regime of the CPT window.

or dominates accompanied with strong nonlinearities. For convenience of description we refer to these two windows as “CPT windows.” The quantized fields to be controlled are applied within the CPT windows, where the atoms are mainly populated in the dark state and strong nonlinearities are utilized. In the same CPT windows we separate the two-mode squeeze operator from the dark state, and in the different CPT windows we segregate the multimode squeeze operator. The driving fields contribute to the cavity mode parametric interaction strengths the first-order small quantity  $O(\Delta/\Omega)$  ( $\Delta_1 = -\Delta_2 = \Delta$ ,  $\Omega_{1,2} = \Omega$ ) and to the beam-splitter interaction strengths the zero-order quantity  $O(1)$ . By comparison, these interaction strengths are at least one order larger than in the previous dispersive cases. The near-resonantly driven scheme is free from spontaneous emission decoherence since atoms almost stay in a long-lived superposition state.

Our scheme should be distinguished from the electromagnetically induced transparency (EIT) based Kerr interactions. EIT is a special case of CPT, where the probe field Rabi frequency is much weaker than the coupling field Rabi frequency, and the dark state is approximately the ground state coupled by the probe field [11–14]. EIT-based Kerr interactions are established by introducing a cascaded dispersive perturbation (the common or another probe field couples the control-field coupled ground state to an auxiliary state [15–20]) or by tuning the probe field [21]. This leads to a giant enhancement of the Kerr nonlinearities. In sharp contrast, in the present scheme, the atoms are near-resonantly dressed with the same or comparable Rabi frequencies, and the dark state is the coherent superposition of the two equally populated ground states. The subtle effects of the nonlinearities on the quantum correlations are deeply hidden behind the dark resonances [22–24]. Close to or beyond CPT, a dissipation mechanism has been identified for two-mode squeezing of the optical fields [25]. Here we will reveal an essentially different mechanism for the two-mode or multimode squeezing close to CPT. The mechanism is based on the two-mode two-photon resonances with the dressed transitions between the second adjacent dark states. By this mechanism, the two-mode interaction strengths are at least one order larger than in the usual dispersive interactions [6–9].

This paper is organized as follows. In Sec. II we describe the physical background on which our scheme is based by recalling briefly the CPT effect and the nonlinearities within the CPT windows. Section III presents the two-mode parametric interaction of the two quantized fields in a common CPT window, and shows that a unitary two-mode squeeze operator is separated out from the degrees of freedom of the near-resonant atoms. The coherence effects on the two-mode parametric interaction are analyzed and the fluctuation spectra of the output fields are presented. In Sec. IV we derive the four-mode parametric interactions within two CPT windows and show the generation of the unitary four-mode squeeze operator. The four-mode quantum correlation is also calculated. Finally, the conclusion is given in Sec. V.

## II. CPT AND NONLINEARITIES

Our purpose is to study the interactions within the CPT windows of dressed three-level atoms in  $\Lambda$  configuration, as shown in Fig. 1(a). In order to clarify the physics, we first describe the CPT windows. The atoms have two metastable states  $|1\rangle$  and  $|2\rangle$  and an excited state  $|3\rangle$ . Two coherent fields of frequencies  $\omega_1$  and  $\omega_2$  interact with the atoms on the electronic-dipole allowed transitions  $|1\rangle \leftrightarrow |3\rangle$  and  $|2\rangle \leftrightarrow |3\rangle$ , respectively. The transition  $|1\rangle \leftrightarrow |2\rangle$  is electronic-dipole forbidden. The master equation for the density operator  $\rho$  of the atom-field system is derived in the dipole approximation and in the frame rotating at the dressing field frequencies as [1,2]

$$\dot{\rho} = -\frac{i}{\hbar}[H_0, \rho] + \mathcal{L}\rho, \quad (1)$$

where the Hamiltonian takes the form

$$H_0 = \sum_{l=1,2} \hbar(\Delta_l \sigma_{ll} + \Omega_l \sigma_{3l} + \Omega_l^* \sigma_{l3}). \quad (2)$$

In the above formulas,  $\hbar$  is the Planck constant.  $\sigma_{kl} = |k\rangle\langle l|$  are the projection operators for  $k = j$  and the spin-flip operators for  $k \neq l$ .  $\Delta_l = \omega_l - \omega_{3l}$  are the detunings of the driving field circular frequencies  $\omega_l$  with respect to the atomic transition circular frequencies  $\omega_{3l}$ . The Rabi frequencies are

defined as  $2\Omega_l = \mu_{l3}E_l/\hbar$ , where  $\mu_{l3}$  are the electric dipole moments and  $E_l$  are the electric amplitudes of the driving fields. The damping term in Eq. (1) takes the form [1]  $\mathcal{L}\rho = \sum_{l=1,2} \gamma_l \mathcal{L}_{\sigma_{l3}}\rho$ , where  $\mathcal{L}_{\sigma_{l3}}\rho$  describes the atomic decays with rates  $2\gamma_l$ , and  $\mathcal{L}_o\rho = 2\rho o^\dagger - o^\dagger o\rho - \rho o^\dagger o$ ,  $o = \sigma_{13}, \sigma_{23}$ .

In order to show clearly the CPT effect, we introduce the superposition states of the metastable states

$$\begin{aligned} |b\rangle &= (\Omega_1^*|1\rangle + \Omega_2^*|2\rangle)/\tilde{\Omega}, \\ |d\rangle &= (\Omega_2|1\rangle - \Omega_1|2\rangle)/\tilde{\Omega}, \end{aligned} \quad (3)$$

where we have defined  $\tilde{\Omega} = \sqrt{|\Omega_1|^2 + |\Omega_2|^2}$ . Using the superposition states, on resonance  $\Delta_{1,2} = 0$ , we rewrite the Hamiltonian (2),

$$H_0 = \hbar\tilde{\Omega}(\sigma_{b3} + \sigma_{3b}), \quad (4)$$

where  $\sigma_{b3} = |b\rangle\langle 3|$  and  $\sigma_{3b} = |3\rangle\langle b|$  are the spin flip operators involving the  $|b\rangle$  state. Only the superposition state  $|b\rangle$  is coupled to the excited state  $|3\rangle$ , while  $|d\rangle$  decouples from the coherent interaction. The stimulated and spontaneous transitions  $|b\rangle \leftrightarrow |3\rangle$  and  $|3\rangle \rightsquigarrow |d\rangle$  act as successive optical pumping, through which the atoms are driven into  $|d\rangle$ . Since there is no population transfer out of  $|d\rangle$ , all population is accumulated in  $|d\rangle$  after several radiative lifetimes. For this reason, the state  $|d\rangle$  is usually called the dark state. This effect is usually referred to as the dark resonance, which underlies CPT. On resonance, we can obtain the atomic coherence for the metastable states as

$$\rho_{12} = -\frac{\Omega_1^*\Omega_2}{|\Omega_1|^2 + |\Omega_2|^2}, \quad (5)$$

which reaches its maximum  $|\rho_{12}| = \frac{1}{2}$  for  $|\Omega_1| = |\Omega_2|$ . At this time, the fields decouple from the system when the atoms are trapped into a dark state entirely. On exact resonance, the medium of the atoms are transparent to the dressing fields.

Generally, the responses of the atoms to the dressing fields are described by the susceptibilities  $\chi_l = -\mu_{l3}\rho_{3l}/(\epsilon_0 E_l)$ , which are written in the form

$$\chi_1 = A_1|\Omega_2|^2, \quad \chi_2 = A_2|\Omega_1|^2, \quad (6)$$

with the complex parameters  $A_{1,2}$  being functions of  $|\Omega_{1,2}|^2$  and being given in Appendix A. The imaginary and real parts of the susceptibilities describe the absorption and the dispersion of the atoms, respectively. It is clear that the susceptibilities have deep dependences on the field intensities  $|\Omega_{1,2}|^2$ . Plotted in Fig. 1(b) are the imaginary part  $\text{Im}\chi_1$  and real part  $\text{Re}\chi_1$  of the susceptibility in unit of  $|\mu_{13}|^2/(\epsilon_0\hbar)$  relative to the detuning  $\Delta_1/\gamma$  for given dressing field intensities  $\Omega_{1,2} = 5\gamma$ . Here we have assumed that  $\Delta_2 = -\Delta_1$  and  $\gamma_{1,2} = \gamma$ , and the same assumption is taken throughout the present article. When the driving fields are tuned from the exact dark-state resonance ( $\Delta_1 = \Delta_2 = 0$ ) by the detunings  $\Delta_1 = -\Delta_2 = \Delta \neq 0$ , two frequency windows are opened, which locate at  $\omega_1 = \omega_{31}$  and  $\omega_2 = \omega_{32}$ , respectively, and which are named the CPT windows, as in the Introduction. Shown in Fig. 1(b) is the CPT window at  $\omega_1 = \omega_{31}$ . The width for the CPT window is determined by  $\Delta_1 = -\Delta_2 = \pm 5\gamma$ , at which the absorption  $\text{Im}\chi_1$  takes its maximal value. This is described in terms of the populations of the dark state as below. When CPT windows are much wider than

the bandwidths of the dressing and applied fields, within the CPT windows, the absorption remains negligibly weak while dispersion is remarkably large compared with the usual case.

In order to show the features of the present system, we introduce the ratio of the dispersion to absorption,

$$\eta_l = \frac{\text{Re}\chi_l}{\text{Im}\chi_l}, \quad \eta_2 = -\eta_1 \quad (l = 1, 2). \quad (7)$$

Shown in Fig. 1(c) is the dependence of the nonlinear parameter  $\eta_1$  versus the normalized detuning  $\Delta_1/\gamma$ . It is noted that, for small detunings  $|\Delta_1| \rightarrow 0$ , the ratios are extremely large,  $|\eta_1| \rightarrow \infty$ . This indicates that the dressing fields experience negligible absorptions but strong nonlinearities close to the dark resonance. In what follows, we tune the fields to be controlled within the CPT windows and analyze their interactions with the CPT atoms. Taking advantage of the characteristics of the CPT system, we engineer the squeeze operators which are independent of the atomic degrees of freedom. For this purpose we will concentrate on the interactions of the applied fields within the CPT windows (i.e., close to the dark-state resonance) throughout this article.

### III. TWO-MODE SQUEEZING IN CPT WINDOW

Now we turn to discussing the interaction of the CPT atoms with two applied fields. The scheme and the corresponding mechanism are sketched in Fig. 2. Shown in Fig. 2(a) is the simultaneous coupling of the two applied fields  $a_{1,2}$  to a common transition  $|1\rangle \leftrightarrow |3\rangle$ . Figure 2(b) describes the case in which the circular frequencies  $\nu_{1,2}$  of these two applied fields are confined within the CPT windows. Depicted in Fig. 2(c) are the two-photon transitions between the second adjacent dark states. Since the absorption of the cavity fields is negligible and the dispersion is giant, the quantized fields will be in strong interactions with the CPT atoms. The Hamiltonian for the interaction of the cavity fields  $a_{1,2}$  with the atom [1,2],

$$H_I = \sum_{l=1,2} \hbar(\delta_l a_l^\dagger a_l + g_l a_l \sigma_{31} + g_l^* \sigma_{13} a_l^\dagger), \quad (8)$$

is added to the Hamiltonian  $H_0$  in the master equation (1) and the cavity loss  $\sum_{l=1}^2 \kappa_l \mathcal{L}_{a_l}\rho$  is added to  $\mathcal{L}\rho$  in the master equation (1) ( $2\kappa_{1,2}$  are the cavity loss rates). In Eq. (8), there is the remaining free term in the frame rotating at the dressing field frequency  $\omega_1$ .  $a_l$  and  $a_l^\dagger$  are the annihilation and creation operators for the cavity modes, and  $g_l$  are the strengths of interactions of the  $l$ th cavity fields with the atoms, respectively.  $\delta_{1,2} = \nu_{1,2} - \omega_1$  are the cavity mode resonance circular frequencies  $\nu_{1,2}$  with respect to the driving field circular frequency  $\omega_1$ . So far, involved in the present scheme is a set of different but adjacent frequencies. We show them in Fig. 3 for clear discrimination, including the frequencies  $\nu_{3,4}$  of the applied fields  $a_{3,4}$  that will be considered in the next section. The frequencies on the left and right parts center at  $\omega_{31}$  and  $\omega_{32}$ , respectively. Either part serves for the two-mode interactions, while both parts are for the four-mode interactions as in the next section.

(i) *Dressed atomic states.* It turns out to be most convenient to use dressed atomic states to show the mechanism for the interaction of the quantized fields with the CPT atoms when

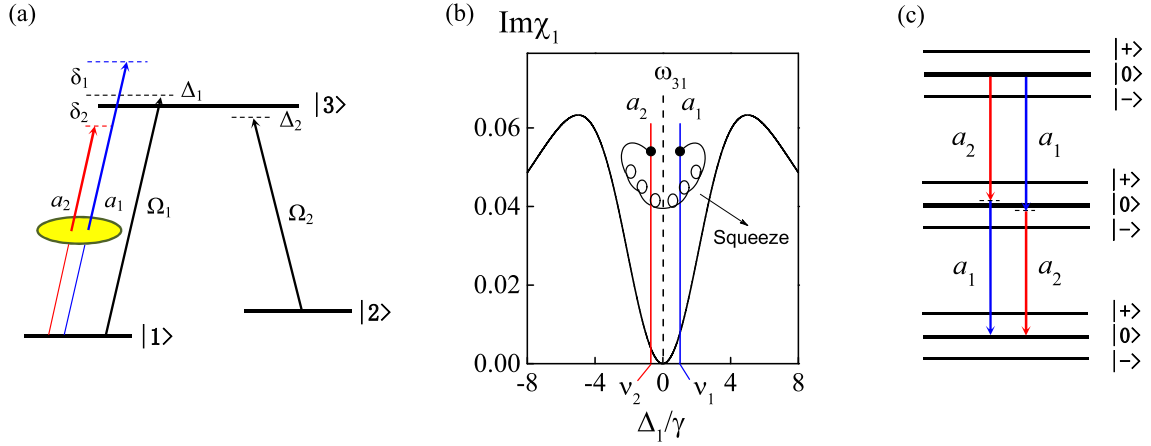


FIG. 2. Interaction of two quantized fields  $a_{1,2}$  with the CPT atom within a common CPT window at  $\omega_{31}$ . (a) Diagram showing the application of two cavity fields  $a_{1,2}$  to the  $|1\rangle \leftrightarrow |3\rangle$  transition. (b) The absorption  $\text{Im}\chi_1$  (dip curve) in units of  $|\mu_{13}|^2/(\epsilon_0\hbar)$  vs the normalized detuning  $\Delta_1/\gamma$  ( $\Delta_2 = -\Delta_1$ ) for  $\Omega_{1,2} = 5\gamma$ . The deep dip represents a CPT window that centers at the atomic resonance frequency  $\omega_{31}$ . The frequencies  $\nu_{1,2}$  of cavity modes  $a_{1,2}$  are within the common CPT window and located about  $\omega_1$ . The absorption to the cavity modes  $a_{1,2}$  is negligibly small while the dispersion is very strong. (c) Three adjacent triplets in the two-dimension networks of the composite states of the three-level atom and the two dressing fields. Dressed transitions for the cavity fields  $a_{1,2}$  are far off resonances between the first adjacent pairs of triplets, but on two-photon resonances with the second adjacent dark state  $|0\rangle$ .

the driving fields are strong. We focus on a particular class of conditions  $\Delta_1 = -\Delta_2 = \Delta$  and  $\Omega_{1,2} = \Omega$ , and assume that the Rabi frequencies are equal and much stronger than the atomic and cavity decay rates  $\Omega \gg (\gamma, \kappa_l)$ . After diagonalizing the Hamiltonian  $H_0$ , we obtain the dressed states, which are expressed in terms of the bare atomic states as [26]

$$\begin{aligned} |+\rangle &= \frac{1 + \sin\theta}{2}|1\rangle + \frac{1 - \sin\theta}{2}|2\rangle + \frac{\cos\theta}{\sqrt{2}}|3\rangle, \\ |0\rangle &= -\frac{\cos\theta}{\sqrt{2}}|1\rangle + \frac{\cos\theta}{\sqrt{2}}|2\rangle + \sin\theta|3\rangle, \\ |-\rangle &= \frac{1 - \sin\theta}{2}|1\rangle + \frac{1 + \sin\theta}{2}|2\rangle - \frac{\cos\theta}{\sqrt{2}}|3\rangle, \end{aligned} \quad (9)$$

where we have defined  $\cos\theta = \frac{\sqrt{2}\Omega}{\bar{\Omega}}$ ,  $\sin\theta = \frac{\Delta}{\bar{\Omega}}$ , and  $\bar{\Omega} = \sqrt{\Delta^2 + 2\Omega^2}$  (generalized Rabi frequency for the present case). In the dressed states representation, the dressed three-level atom has its Hamiltonian in the free form  $H_0 = \hbar\bar{\Omega}(\sigma_{++} - \sigma_{--})$ , where  $\sigma_{\pm\pm} = |\pm\rangle\langle\pm|$ . It indicates that these dressed states  $|0\rangle$  and  $|\pm\rangle$  have the equally spaced eigenvalues  $0, \pm\hbar\bar{\Omega}$ . It should be noted that once  $\Delta = 0$  ( $\sin\theta = 0$ ,  $\cos\theta = 1$ ), the state  $|0\rangle$  is simply reduced to the dark state  $|d\rangle = \frac{1}{\sqrt{2}}(-|1\rangle + |2\rangle)$ , as in Eq. (3). Expressing the atomic relaxations in terms of the dressed atomic states, we obtain the steady-state populations  $\langle\sigma_{00}\rangle = \frac{\cos^4\theta}{1+3\sin^4\theta}$  and  $\langle\sigma_{\pm\pm}\rangle = \frac{1}{2}(1 - \langle\sigma_{00}\rangle)$ . If  $\Delta = 0$ , we have  $\langle\sigma_{00}\rangle = 1$  and  $\langle\sigma_{\pm\pm}\rangle = 0$ . Once again, it shows that, when  $\Delta = 0$ , the atoms are trapped in the dark state  $|0\rangle$ . As the normalized detuning rises to  $|\Delta|/\Omega = 1$

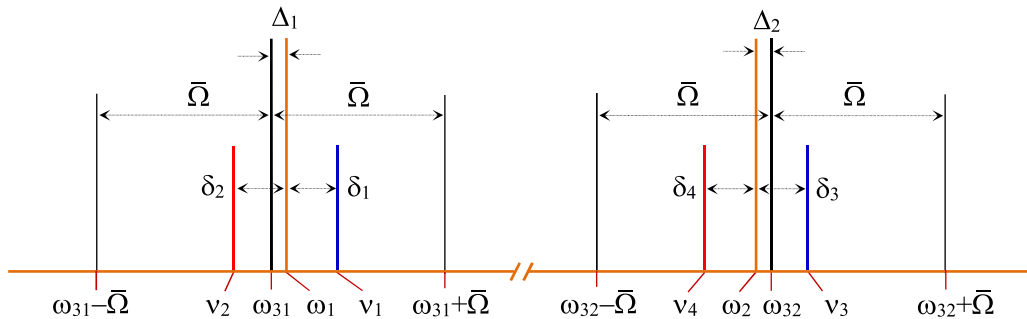


FIG. 3. Diagrammatic sketch of various frequencies and detunings along the frequency axis. The left and right parts, which center at the atomic resonance frequencies  $\omega_{31}$  and  $\omega_{32}$  respectively, are related to the dipole-allowed transitions  $|1\rangle \leftrightarrow |3\rangle$  and  $|2\rangle \leftrightarrow |3\rangle$  respectively. The dressing field frequencies  $\omega_{1,2}$  are very close to  $\omega_{31}$  and  $\omega_{32}$  respectively by the detunings  $\Delta_{1,2}$ . The frequencies  $\nu_{1,2}$  ( $\nu_{3,4}$ ) of the applied fields coupled to the transition  $|1\rangle \leftrightarrow |3\rangle$  ( $|2\rangle \leftrightarrow |3\rangle$ ) are located symmetrically about  $\omega_1$  ( $\omega_2$ ) with the detunings  $\delta_{1,2}$  ( $\delta_{3,4}$ ), respectively.  $\omega_{31} \pm \bar{\Omega}$  ( $\omega_{32} \pm \bar{\Omega}$ ) are respectively the frequencies of the shifted dressed states  $|\pm\rangle$  associated with the transition  $|1\rangle \leftrightarrow |3\rangle$  ( $|2\rangle \leftrightarrow |3\rangle$ ). Essentially,  $\omega_{31} + \bar{\Omega}$  and  $\omega_{32} + \bar{\Omega}$  ( $\omega_{31} - \bar{\Omega}$  and  $\omega_{32} - \bar{\Omega}$ ) correspond to a common dressed state  $|+\rangle$  ( $|-\rangle$ ) of the excited state  $|3\rangle$ . But in order to show clearly the level splittings relative to different transitions, we attach the split frequencies  $\omega_{3l} \pm \bar{\Omega}$  (corresponding to the dressed states  $|\pm\rangle$  respectively) to about the respective central levels  $\omega_{3l}$  ( $l = 1, 2$ ). The spacing  $\bar{\Omega}$  measures the deviations of the dressed states from the dark states.



we have  $\langle\sigma_{00}\rangle = \langle\sigma_{\pm\pm}\rangle = \frac{1}{3}$ . At this time, the absorption to the dressing fields reaches its maximum, by which the width for the CPT window is determined. For the exact CPT case, the fields undergo neither absorption nor dispersion, and so no squeezing occurs. Instead, in what follows we will focus on the near-resonance conditions  $\Delta \neq 0$  but  $|\Delta| \ll \bar{\Omega}$ . Under such conditions, the atoms are very slightly excited, and then we have two CPT windows at the atomic resonance frequencies  $\omega_{31}$  and  $\omega_{32}$ . What we are interested in is the atom-field interactions within the CPT windows.

(ii) *Two-mode interaction within a common CPT window.* We are now in the position to show the two-mode interaction with the dressed atoms. To do so, we make once again a unitary transformation with  $H_0 + \sum_{l=1,2} \hbar \delta_l a_l^\dagger a_l$ , and then a rotating-wave approximation. Now we have the interaction Hamiltonian

$$\begin{aligned} H_I' = & \hbar \sigma_{+0} e^{i\bar{\Omega}t} (G_1 a_1 e^{-i\delta_1 t} + G_2 a_2^\dagger e^{i\delta_2 t}) \\ & + \hbar \sigma_{0-} e^{i\bar{\Omega}t} (\tilde{G}_1 a_1 e^{-i\delta_1 t} + \tilde{G}_2 a_2^\dagger e^{i\delta_2 t}) \\ & + \text{H.c.}, \end{aligned} \quad (10)$$

where  $\sigma_{+0} = |+\rangle\langle 0|$  and  $\sigma_{0-} = |0\rangle\langle -|$  are the spin flip operators for the dressed-state atomic states, H.c. is Hermitian conjugate, and we have used  $G_1 = -g_1 \cos^2 \theta/2$ ,  $G_2 = g_2^* (1 + \sin \theta) \sin \theta/2$ ,  $\tilde{G}_1 = g_1^* (1 - \sin \theta) \sin \theta/2$ ,  $\tilde{G}_2 = g_2 \cos^2 \theta/2$ . It is easily seen from Eq. (10) that two cavity modes are in resonant interactions with the corresponding dressed transitions once  $\delta_{1,2} = \pm \bar{\Omega}$ . For that case, the squeezing occurs due to engineered dissipation, which has been presented in [25]. Here we consider the different case, however, in which the cavity fields are far off resonances with the first adjacent dark states but on two-photon resonances with the second dark states, as shown in Fig. 2(c). Then, we tune the cavity fields  $\delta_{1,2} = \pm \delta + \bar{\delta}/2$ , and assume that  $(\Omega, \delta) \gg |\delta - \bar{\Omega}| \gg (\bar{\delta}, |g_l \langle a_l \rangle|, \gamma_l, \kappa_l)$ ,  $l = 1, 2$ . In Appendix B we include  $N$  atoms and derive the effective Hamiltonian in the form

$$H_{12} = \hbar (\xi^* a_1 a_2 + \xi a_1^\dagger a_2^\dagger), \quad (11)$$

with the two-mode coupling coefficient

$$\xi = \frac{g_1^* g_2^* N}{2\sqrt{2}\bar{\delta}} \left( \frac{\Delta}{\Omega} \right), \quad (12)$$

where  $\bar{\delta} = \sqrt{2}\Omega - \delta$  is the detuning of the cavity field from the dressed transition. The Hamiltonian (11) is no longer dependent on the atomic spin projection operators and spin-flip operators. This is one of our key results in the present work.

(iii) *Analysis of atomic coherence effects.* Before we proceed to further discussion, it is interesting for us to summarize the characteristic features of the two-mode interaction within the common CPT window.

(a) The parametric down-conversion interaction happens for the cavity fields when the dressing fields are close to resonances with the atoms. In this case, it is the coherent effects that lead to absorption cancellation and dispersion enhancement. This is in sharp contrast to the previous cases, e.g., Ref. [7], in which all fields (including the dressing and cavity fields) are all far off resonances, and the dispersion is

greatly reduced although the dispersion is dominant over the absorption.

(b) The ground states give the complete contribution although only one ground state  $|1\rangle$  is directly coupled to the cavity fields  $a_{1,2}$ . It seems that only 50% population is involved since the other ground state  $|2\rangle$  is not coupled directly. However, the dark state as the coherent superposition of the ground states behaves as a single state and thus contributes the entire population ( $\langle\sigma_{00}\rangle \approx 1$ ) to the two-mode interaction strength  $|\xi|$ .

(c) CPT-based nonlinearities boost the two-mode parametric interaction strength compared with the previous schemes based on the dispersive interactions. The two-mode interaction strength displays a dependence on the first-order small quantity  $O(\Delta/\Omega)$  of the dressing fields ( $|\Delta|/\Omega \ll 1$ ). This is completely different from the case in dispersive interactions (e.g., in Refs. [3,7]), where there is a second-order dependence on the corresponding small quantities  $O(\Omega_k/\Delta_k)O(\Omega_l/\Delta_l)$ , where  $\Omega_l/|\Delta_l| \ll 1$ . This means that, for the present near-resonant case, the two-mode interaction strength is raised by at least one order of magnitude. Once the dressing fields  $E_{1,2}$  are too far from the CPT window center or the signal fields  $a_{1,2}$  become too strong, feedback and saturation effects will spoil perfect squeezing, but those considerations are beyond the scope of the present work.

(iv) *Squeeze operators and correlation spectra.* The effective parametric interaction (11) means that the two cavity modes  $a_{1,2}$  in the CPT window [Figs. 2(b) and 2(c)] can be prepared in the two-mode squeezed state. When the cavity loss rates are negligibly small, the two-mode state evolves according to the unitary operator

$$S_2(\zeta) = e^{\zeta^* a_1 a_2 - \zeta a_1^\dagger a_2^\dagger}, \quad (13)$$

where we have defined the parameter  $\zeta = i\xi\tau$  with  $\tau$  being the interaction time. Applying it to the vacuum states, we can obtain two-mode squeezed states. This evolution operator is just the two-mode squeeze operator, and  $|\zeta|$  is a squeeze parameter.

By including the cavity losses we can obtain the variance of the internal field mode and of the individual frequency components. By using a definite order  $(a_1^\dagger, a_2^\dagger, a_2, a_1)$  and the correspondences between the  $c$  numbers and the operators  $\alpha_i \leftrightarrow a_i$ ,  $\alpha_i^* \leftrightarrow a_i^\dagger$  ( $i = 1, 2$ ), we derive the set of Langevin equations from the effective nonlinear interaction in Eq. (11) as

$$\begin{aligned} \dot{\alpha}_1 &= -i\epsilon_1^* - \kappa_1 \alpha_1 + |\xi| \alpha_2^* + F_{\alpha_1}, \\ \dot{\alpha}_2 &= -i\epsilon_2^* - \kappa_2 \alpha_2 + |\xi| \alpha_1^* + F_{\alpha_2}, \end{aligned} \quad (14)$$

together with those for  $\alpha_{1,2}^*, \epsilon_{1,2}^*$  are the average amplitudes of the input fields, and we have assumed that  $\xi = |\xi|e^{i\phi}$  and have substituted  $a_2$  for  $a_2 e^{-i\phi}$  to match standard notation [2,27]. The  $F$  terms are noises with zero means and correlations  $\langle F_x(t)F_y(t') \rangle = D_{xy}\delta(t-t')$ ,  $D_{xy} = D_{yx}$ , and  $D_{x^*y^*} = D_{xy}^*$ . Nonzero diffusion coefficients read as  $D_{\alpha_1\alpha_2} = D_{\alpha_1^*\alpha_2^*} = |\xi|^2$ . We use the quadrature operators for the fields

$$x_l = a_l + a_l^\dagger, \quad p_l = -i(a_l - a_l^\dagger) \quad (15)$$

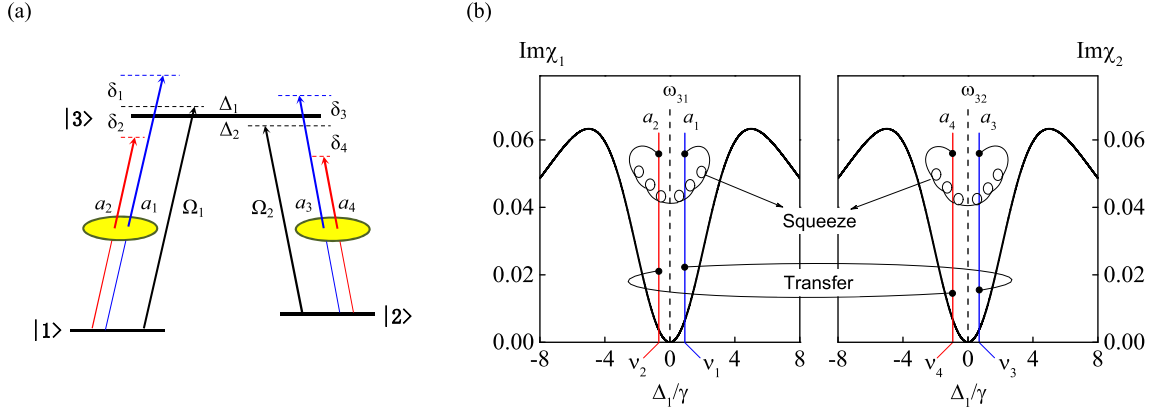


FIG. 4. Interaction of four quantized fields  $a_{1-4}$  with the CPT atom. (a) Diagram showing the couplings of a pair of the cavity modes  $a_{1,2}$  ( $a_{3,4}$ ) to the  $|1\rangle \leftrightarrow |3\rangle$  ( $|2\rangle \leftrightarrow |3\rangle$ ) transition in  $\Lambda$  configuration. (b) The absorption  $\text{Im}\chi_1$  and  $\text{Im}\chi_2$  (dip curves) in units of  $|\mu_{13}|^2/(\epsilon_0\hbar)$  and  $|\mu_{23}|^2/(\epsilon_0\hbar)$  vs the normalized detuning  $\Delta_1/\gamma$  ( $\Delta_2 = -\Delta_1$ ) for  $\Omega_{1,2} = 5\gamma$ . The two deep dips center at the atomic resonance frequencies  $\omega_{31}$  and  $\omega_{32}$ , respectively, and stand for the coupled CPT windows. The frequencies  $\nu_{1,2}$  of cavity modes  $a_{1,2}$  are within the CPT window at  $\omega_{31}$ , while the frequencies  $\nu_{3,4}$  of cavity modes  $a_{3,4}$  are located within the CPT window at  $\omega_{32}$ . All cavity fields  $a_{1-4}$  have large dispersion but negligibly small absorption. The cavity modes in the same CPT window are in down-conversion interaction (for squeezing generation) with each other, while those two modes in different CPT windows and linked by an arc are in beam-splitter interaction (for quantum state transfer) with each other.

to define a pair of the two-mode quadrature operators as

$$X_2 = \frac{1}{\sqrt{2}}(x_1 + x_2), \quad P_2 = \frac{1}{\sqrt{2}}(p_1 + p_2), \quad (16)$$

which satisfy the commutation relation  $[X_2, P_2] = 2i$ . When the variance of any quadrature is less than unity,  $\langle(\delta X_2)^2\rangle < 1$  or  $\langle(\delta P_2)^2\rangle < 1$ , the two-mode squeezing occurs [1,2]. Linearizing Eq. (14) we obtain the stability condition  $|\xi| < \sqrt{\kappa_1\kappa_2}$ . For  $\kappa_1 = \kappa_2 = \kappa$ , we can obtain the variances  $\langle(\delta X_2)^2\rangle = \frac{\kappa}{\kappa - |\xi|}$  or  $\langle(\delta P_2)^2\rangle = \frac{\kappa}{\kappa + |\xi|}$ . As  $|\xi| \rightarrow \kappa$ , we have  $\langle(\delta P_2)^2\rangle \rightarrow \frac{1}{2}$ , which means that the squeezing of the internal field mode approaches 50%.

However, this can be surpassed in the individual frequency components of the output field, which have almost ideal squeezing for the zero frequency. What may be measured by a spectrum analyzer following a homodyne detection scheme is the squeezing in the individual frequency components of the output field [2]. By using the input-output relations [27]  $a_l^{\text{in}} + a_l^{\text{out}} = \sqrt{2\kappa_l}a_l$  ( $l = 1, 2$ ) we derive the fluctuation correlation spectra for the output fields

$$\langle\delta O(\omega)\delta O(\omega')\rangle = S_O^{\text{out}}(\omega)\delta(\omega + \omega'), \quad O = X_2, P_2 \quad (17)$$

in Appendix C. The output spectra at zero frequency read

$$S_{X_2}^{\text{out}}(0) = \left( \frac{|\xi| + \sqrt{\kappa_1\kappa_2}}{|\xi| - \sqrt{\kappa_1\kappa_2}} \right)^2, \quad S_{P_2}^{\text{out}}(0) = \left( \frac{|\xi| - \sqrt{\kappa_1\kappa_2}}{|\xi| + \sqrt{\kappa_1\kappa_2}} \right)^2. \quad (18)$$

If the nonlinear coupling vanishes ( $\xi = 0$ ), we have  $S_{X_2}^{\text{out}}(0) = S_{P_2}^{\text{out}}(0) = 1$ , which means that the two cavity fields stay in a coherent state (including the vacuum state). Under general conditions, we have  $1 \leq S_{X_2}^{\text{out}}(0) < \infty$  and  $0 \leq S_{P_2}^{\text{out}}(0) \leq 1$ . Since  $S_{X_2}^{\text{out}}(0)S_{P_2}^{\text{out}}(0) = 1$ , the two cavity fields come to a minimum uncertainty field state. When the two-mode interaction strength matches the cavity damping rates,  $|\xi| \rightarrow \sqrt{\kappa_1\kappa_2}$ ,

we have  $S_{X_2}^{\text{out}} \rightarrow \infty$  and  $S_{P_2}^{\text{out}}(0) \rightarrow 0$ , which means that the quadrature  $P_2^{\text{out}}$  at the output, in principle, can reach ideal squeezing, at the expense of large fluctuations in the output quadrature  $X_2^{\text{out}}$ .

Actually, which quadrature is squeezed depends on the phase of the effective coupling coefficient  $\xi = |\xi|e^{i\phi}$ . If  $\phi \neq 0$ , we need transform back to  $a_2 \rightarrow a_2e^{i\phi}$ . As a comparison, for  $\phi = \pi$ , the sum operators in Eq. (16) are changed to the difference forms  $X_2 = \frac{1}{\sqrt{2}}(x_1 - x_2)$ ,  $P_2 = \frac{1}{\sqrt{2}}(p_1 - p_2)$ , the latter of which is squeezed. Once  $\phi \neq 0, \pi$ , the two-mode quadrature operators that can be squeezed depend on the phase  $\phi$  in a more general form. Now we can take a pair of EPR operators for  $\phi = \pi$  as

$$X = \frac{1}{\sqrt{2}}(x_1 + x_2), \quad P = \frac{1}{\sqrt{2}}(p_1 - p_2), \quad (19)$$

which commute with each other,  $[X, P] = 0$ , and have the same fluctuation spectrum. As a result, when the above stability and matching condition is met,  $|\xi| \rightarrow \sqrt{\kappa_1\kappa_2}$ , we have  $S_X^{\text{out}}(0) + S_P^{\text{out}}(0) \rightarrow 0$ , which corresponds to the EPR entanglement at the zero frequency [4,28].

#### IV. FOUR-MODE SQUEEZING IN COUPLED CPT WINDOWS

Now that we have considered the common CPT window for the two-mode interactions, we extend to the two coupled CPT windows for the multimode interactions.

(i) *Two different kinds of two-mode interactions with the CPT atoms.* On the basis of the above model, we couple the other two cavity fields  $a_{3,4}$  to the other dipole-allowed transition  $|2\rangle \leftrightarrow |3\rangle$ , as shown in Fig. 4(a). The frequencies  $\nu_{3,4}$  of cavity modes  $a_{3,4}$  are close to  $\omega_{31}$ . We can tune the cavity fields such that  $a_{1,2}$  ( $\delta_{1,2} = \nu_{1,2} - \omega_1 \approx \pm\delta$ ) remain within the CPT window at  $\omega_{31}$ , and  $a_{3,4}$  ( $\delta_{3,4} = \nu_{3,4} - \omega_2 \approx \pm\delta$ ) locate in the CPT window at  $\omega_{32}$ , as shown in Fig. 4(b). The absorption of four cavity modes  $a_{1-4}$  is negligible while the

dispersion is very strong. From now on we focus on the same conditions as above,  $(|\Delta|, |\delta|) \ll \Omega$ . Let us list two different cases for two-mode interactions.

(a) Two cavity fields are coupled to one common transition. The case of only the modes  $a_{1,2}$  has been discussed in the above section. Similarly, in the presence of only the modes  $a_{3,4}$ , we can have the same Hamiltonian as (11) except for the substitutions of indices 3 and 4 for 1 and 2, respectively.

(b) Two cavity fields are respectively coupled to different transitions. In the presence of only the  $a_{1,3}$  modes, we follow the same method as above and derive the effective Hamiltonian as

$$H_{13} = \hbar(\xi_{13}a_1a_3^\dagger + \xi_{13}^*a_1^\dagger a_3), \quad (20)$$

where the coupling coefficient is

$$\xi_{13} = \frac{g_1 g_3^* N}{4\delta}. \quad (21)$$

In this case the Hamiltonian (20) indicates that the two cavity fields are in the beam-splitter-like interaction, which leads to the quantum state transfer between  $a_{1,3}$ . In addition to the dependence on the cavity field detunings from the dressed transitions  $\delta$ , the effective coupling strength is not dependent on the factor  $\Delta/\Omega$ . This means that quantum state transfer can occur much more rapidly from one mode to the other than the squeezing generation as above. The same happens for the presence of only the  $a_{2,4}$  modes.

We note that no direct interaction happens between  $a_1$  and  $a_4$  and between  $a_2$  and  $a_3$ . Because of large mismatch of the frequencies  $(|\nu_1 - \nu_4|, |\nu_3 - \nu_2|) \gg |\omega_1 - \omega_2|$ , each pair are neither on two-photon resonances nor on Raman resonances in the dressed atomic picture. Since  $a_1$  and  $a_4$  ( $a_2$  and  $a_3$ ) are not resonant in pairing with the CPT atom, between them there is no longer any direct interaction.

(ii) *Four-mode interaction within the coupled CPT windows.* To sum up, the four modes are simultaneously coupled to the atoms. Combining the above two cases, we can study the interactions of four quantized fields with the CPT atoms. Following the same method as above, one can obtain the effective Hamiltonian for the four-mode interaction as

$$H_{1-4} = \hbar(\xi_{12}a_1a_2 + \xi_{34}a_3a_4 + \xi_{13}a_1a_3^\dagger + \xi_{24}a_2a_4^\dagger) + \text{H.c.}, \quad (22)$$

where we have substituted  $-a_4$  for  $a_4$  and have defined the cross coupling coefficients between the cavity fields as

$$\begin{aligned} \xi_{l,l+1} &= \frac{g_l^* g_{l+1}^* N}{2\sqrt{2}\delta} \left( \frac{\Delta}{\Omega} \right), \quad l = 1, 3, \\ \xi_{l,l+2} &= \frac{g_l^* g_{l+2}^* N}{4\delta}, \quad l = 1, 2. \end{aligned} \quad (23)$$

The effective coupling strengths  $\xi_{12}(=\xi)$  and  $\xi_{13}$  are simply the same as those in Eqs. (12) and (21), respectively, and  $\xi_{34}$  and  $\xi_{24}$  have the same dependences on the system parameters. The four-mode interaction Hamiltonian (22) is independent of the degrees of freedom of the atoms. This is the second part of our main results.

The Hamiltonian (22) shows that all four modes  $a_{1-4}$  are in the loop interactions, which happen alternately in the

parametric amplifier types and in the beam-splitter types. Once squeezing is established between two adjacent modes  $a_{1,2}$  or  $a_{3,4}$ , quantum state transfer between  $a_{1,3}$  or  $a_{2,4}$  will lead to nonclassical correlations of the two squeezed modes to the third mode. In particular, take  $a_{1-3}$  as an example. The cavity mode  $a_1$  entangles with  $a_2$  and transfers immediately its own state to  $a_3$ . As a consequence, the cavity modes  $a_{1-3}$  are prepared into a squeezed state.

(iii) *Four-mode squeeze operator and quantum correlations.* If the cavity losses are negligibly small, the four-mode field evolves according to the unitary operator

$$S_4(\zeta) = e^{\zeta_{12}^* a_1 a_2 + \zeta_{34}^* a_3 a_4 + \zeta_{13} a_1 a_3^\dagger + \zeta_{24} a_2 a_4^\dagger - \text{H.c.}}, \quad (24)$$

where we have defined the parameters  $\zeta = (\zeta_{12}, \zeta_{34}, \zeta_{13}, \zeta_{24})$  and  $\zeta_{kl} = i\xi_{kl}\tau$ . The evolution operator is just the multimode squeeze operator. Naturally, this general squeeze operator is also independent of the atomic degrees of freedom. Differently from the two-mode case, there is not only the  $a_1 a_2$  form, but also the other  $a_1 a_3^\dagger$  form. The former is responsible for the squeezing generation while the latter corresponds to the squeezing transfer. When it is applied to the vacuum state, the squeezing creation and the state transfer combine to generate multimode squeezed states.

The noise correlations of the four fields are calculated by using the effective Hmailtonian (22) and including the cavity loss  $\sum_{l=1}^4 \kappa_l \mathcal{L}_{a_l} \rho$  in the master equation ( $2\kappa_{1-4}$  are the cavity loss rates). We choose a definite operator order,  $(a_1^\dagger, a_2^\dagger, a_3^\dagger, a_4^\dagger, a_4, a_3, a_2, a_1)$ , and use the correspondences between the  $c$  numbers and operators  $\alpha_k \leftrightarrow a_k$ ,  $\alpha_k^* \leftrightarrow a_k^\dagger$  ( $k = 1-4$ ). For the sake of simplicity we assume  $-i\xi_{kl}$  to be positive, then we substitute  $\xi_{kl}$  for  $-i\xi_{kl}$  and match the standard notation as for the two-mode case. The set of Langevin equations are derived as follows:

$$\begin{aligned} \dot{\alpha}_1 &= -i\epsilon_1^* - \kappa_1 \alpha_1 + \xi_{13} \alpha_3 + \xi_{12} \alpha_2^* + F_{\alpha_1}, \\ \dot{\alpha}_2 &= -i\epsilon_2^* - \kappa_2 \alpha_2 + \xi_{24} \alpha_4 + \xi_{12} \alpha_1^* + F_{\alpha_2}, \\ \dot{\alpha}_3 &= -i\epsilon_3^* - \kappa_3 \alpha_3 + \xi_{13} \alpha_1 + \xi_{34} \alpha_4^* + F_{\alpha_3}, \\ \dot{\alpha}_4 &= -i\epsilon_4^* - \kappa_4 \alpha_4 + \xi_{24} \alpha_2 + \xi_{34} \alpha_3^* + F_{\alpha_4}, \end{aligned} \quad (25)$$

together with those for  $\alpha_{1-4}^*$ .  $\epsilon_{1-4}^*$  are the average amplitudes of the input fields. The nonzero diffusion coefficients are  $D_{\alpha_2 \alpha_1} = \xi_{12}$ ,  $D_{\alpha_4 \alpha_3} = \xi_{34}$ ,  $D_{xy} = D_{yx}$ , and  $D_{x^* y^*} = D_{xy}^*$ . To investigate the multimode correlations, we first define the quadrature operators for each cavity mode as in Eq. (15). Then the collective quadrature operators for four modes can be defined as

$$\begin{aligned} X_4 &= \frac{1}{2}(x_1 - x_2 - x_3 + x_4), \\ P_4 &= \frac{1}{2}(p_1 + p_2 - p_3 - p_4). \end{aligned} \quad (26)$$

When the variance of any quadrature is less than unity,  $\langle (\delta X_4)^2 \rangle < 1$  or  $\langle (\delta P_4)^2 \rangle < 1$ , the multimode squeezing appears [1,2]. The measurable quantities for the optical fields outside the cavity are the fluctuation correlation spectra. For the case of four modes, the analytical calculation can be obtained in the same way as for the two-mode case in Appendix C. It turns out to be relatively complicated, and here we present the numerical results as follows.

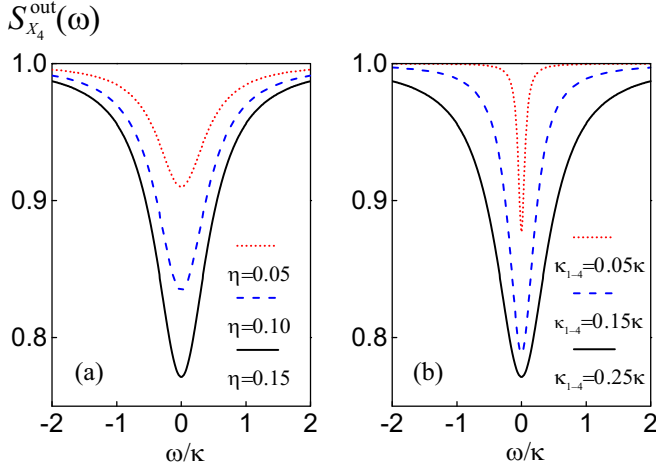


FIG. 5. (a) The four-mode correlation spectra  $S_{X_4}^{out}(\omega) [=S_{P_4}^{out}(\omega)]$  for different values of  $\eta = \Delta/\sqrt{2}\Omega$ : 0.05 (dot line), 0.10 (dash line), and 0.15 (solid line); and fixed  $\kappa_{1-4} = 0.25\kappa$ . (b) The four-mode correlation spectra  $S_{X_4}^{out}(\omega) [=S_{P_4}^{out}(\omega)]$  for different rates of cavity damping  $\kappa_{1-4}$ :  $0.05\kappa$  (dot line),  $0.15\kappa$  (dash line), and  $0.25\kappa$  (solid line); and for fixed  $\eta = 0.15$ . The other parameters are chosen as  $C_{1-4} = 60$  and  $\delta = 5$ .

$S_{X_4}^{out}(\omega)$  and  $S_{P_4}^{out}(\omega)$ , by which we denote the output spectra for  $O = X_4, P_4$ , respectively, are obtained from the general definition as in Eq. (17). Here we rescale the decay rates, detunings, Rabi frequencies, and Fourier frequency in units of a rate parameter  $\kappa$ , in MHz. We define the cooperativity parameters  $C_l = g_l^2 N / \kappa_l^2$ . Plotted in Fig. 5 are the four-mode correlation spectra  $S_{X_4}^{out}(\omega) [=S_{P_4}^{out}(\omega)]$  (a) for different values of the parameter  $\eta = \Delta/\sqrt{2}\Omega$  and (b) for different values of the cavity damping  $\kappa_{1-4}$ . The chosen parameters are listed in the figure caption. It is seen that for various choices of parameters, the fluctuation spectrum drops below the standard quantum limit 1. This means that the four-mode quadratures  $X_4^{out}$  and  $P_4^{out}$  at the output have the reduced fluctuations. The numerical results verify the prediction as above. The direct generation of squeezing occurs between the cavity fields  $a_{1,2}$  and between  $a_{3,4}$ , while quantum state transfer happens between the cavity fields  $a_{1,3}$  and between  $a_{2,4}$ . The combination of the squeezing with the transfer leads to the four-mode squeezing. Generally, the degree of squeezing depends strongly on various parameters such the normalized detunings and the cavity damping rates. Like the two-mode case, the optimal squeezing occurs when the interaction strength matches the cavity damping rates. Once we tune the dressing fields  $E_{1,2}$  to be far off the CPT window center or increase the signal fields  $a_{1-4}$ , feedback and saturation effects will prevent the squeezing from generating. Those considerations go beyond the scope of the present work.

We also note that the mechanism of the present scheme is essentially different from the entanglement swapping for continuous variables [29,30]. For the present case, squeezing occurs for four modes through the combination of two mechanisms: parametric down-conversion interactions between  $a_1$  and  $a_2$  and between  $a_3$  and  $a_4$ , and the beam-splitter-like

interactions between  $a_1$  and  $a_3$  and between  $a_2$  and  $a_4$ . These two kinds of interactions are in a successively cascaded, closed contour. For the latter, two initial pairs of entangled optical fields are produced independently, e.g., from two nondegenerate optical parametric amplifiers. Through implementing the direct measurement of the Bell-state between two optical fields from their respective initial entanglement pairs, the remaining two optical fields, which have never directly interacted with each other, become entangled.

As possible experimental realization we can use cold atoms confined in a magneto-optical trap. A great number of atomic structures can be used as candidates for the present scheme, for example, the  $^{85}\text{Rb}$   $D_1$  (795 nm) transition hyperfine structure. The two lower levels are the ground state hyperfine levels  $|1\rangle = |5^2S_{1/2}, F=1\rangle$  and  $|2\rangle = |5^2S_{1/2}, F=2\rangle$ , separated from each other by 3 GHz, while the upper state is the excited state hyperfine level  $|3\rangle = |5^2P_{1/2}, F=2\rangle$ . The other excited state hyperfine level  $|5^2P_{1/2}, F=1\rangle$  is 362 MHz below  $|3\rangle$  and has a negligible influence. The cavity parameters of Ref. [31] can be used for this purpose: the waist is  $w \sim 35 \mu\text{m}$ , homogeneous laser beams have width  $d \sim 50 \mu\text{m}$ , and the interaction volume is  $10^{-7} \text{ cm}^3$ . A density of  $10^{11} \text{ cm}^{-3}$  (small enough to prevent coherence losses due to collisions) corresponds to the number of atoms  $N \sim 10^4$ . Taking  $\Delta/\Omega \sim 1/10$  and  $\delta \sim 50g$ , we have approximately the effective two-mode interaction strengths  $(|\xi_{12}|, |\xi_{34}|) \sim 10g$  and  $(|\xi_{13}|, |\xi_{24}|) \sim 10(|\xi_{12}|, |\xi_{34}|)$ . This is just a rather conservative estimate of parameters and so there is a wide range of possibilities for the realization of the present scheme.

## V. CONCLUSION

In conclusion, we have shown a method of isolating out a unitary field-squeeze operator from the degrees of freedom of the near-resonantly dressed atoms. The scheme is based on the atom-field interactions within the coherent population trapping (CPT) windows, which are opened when two optical fields interact with the three-level atoms in the  $\Lambda$  configuration, and in which the absorption is negligibly small while the dispersion is remarkably large due to the atomic coherence. Two fields used in one common CPT window are in parametric down-conversion interaction with each other, while the two fields applied in different CPT windows are in beam-splitter interactions. As a result, a unitary two-mode or four-mode squeeze operator can be separated from the degrees of freedom of atoms. At the same time, the interaction strengths are at least one order larger than in the conventional dispersive cases. The CPT-based near-resonant scheme is free from spontaneous emission decoherence because the atoms are hardly excited and instead stay dominantly in the coherent superposition of the ground states.

## ACKNOWLEDGMENTS

This work is supported by the National Natural Science Foundation of China (Grants No. 61178021 and No. 61875067) and by the National Basic Research Program of China (Grant No. 2012CB921604).



### APPENDIX A: STEADY-STATE SOLUTIONS OF THE DENSITY MATRIX ELEMENTS

We derive the equations of motion for the density matrix elements from Eq. (1) as follows:

$$\begin{aligned}\dot{\rho}_{31} &= -\Gamma_{13}\rho_{31} - i\Omega_1(\rho_{11} - \rho_{33}) - i\Omega_2\rho_{21}, \\ \dot{\rho}_{32} &= -\Gamma_{23}\rho_{32} - i\Omega_2(\rho_{22} - \rho_{33}) - i\Omega_1\rho_{12}, \\ \dot{\rho}_{21} &= -\Gamma_{12}\rho_{21} - i\Omega_2^*\rho_{31} + i\Omega_1\rho_{23}, \\ \dot{\rho}_{11} &= 2\gamma_1\rho_{33} - i\Omega_2^*\rho_{31} + i\Omega_1\rho_{13}, \\ \dot{\rho}_{22} &= 2\gamma_2\rho_{33} - i\Omega_2^*\rho_{32} + i\Omega_2\rho_{23},\end{aligned}\quad (\text{A1})$$

together with the related complex conjugates and the closure relation  $\rho_{11} + \rho_{22} + \rho_{33} = 1$ . We have defined  $\Gamma_{12} = i(\Delta_2 - \Delta_1)$ ,  $\Gamma_{13} = \gamma_1 + \gamma_2 - i\Delta_1$ , and  $\Gamma_{23} = \gamma_1 + \gamma_2 - i\Delta_2$ . At steady state, the nondiagonal elements  $\rho_{13}$ ,  $\rho_{32}$ , and  $\rho_{12}$  are in a closed set of equations. We solve for them first and then substitute them into the equations of the diagonal elements. After solving for the diagonal elements we substitute them back to the nondiagonal elements. By such steps we derive the susceptibilities in Eq. (6), where the parameters  $A_{1,2}$  are

$$\begin{aligned}A_1 &= \frac{i|\mu_{13}|^2}{\varepsilon_0\hbar V}[\gamma_1(P_1\bar{P}_2 - Q_1\bar{Q}_2) + \gamma_2(P_1\bar{Q}_2 - \bar{P}_1Q_2)], \\ A_2 &= \frac{i|\mu_{23}|^2}{\varepsilon_0\hbar V}[\gamma_2(\bar{P}_1P_2^* - \bar{Q}_1Q_2^*) + \gamma_1(P_2^*\bar{Q}_1 - \bar{P}_2Q_1^*)],\end{aligned}\quad (\text{A2})$$

where we have defined the parameters

$$\begin{aligned}P_1 &= (\Gamma_{12}\Gamma_{23}^* + |\Omega_1|^2)/U, & Q_1 &= |\Omega_2|^2/U, \\ P_2 &= (\Gamma_{12}\Gamma_{13} + |\Omega_2|^2)/U, & Q_2 &= |\Omega_1|^2/U, \\ U &= \Gamma_{12}\Gamma_{13}\Gamma_{23}^* + \Gamma_{12}|\Omega_1|^2 + \Gamma_{23}^*|\Omega_2|^2\end{aligned}\quad (\text{A3})$$

and

$$\begin{aligned}\bar{P}_{1,2} &= 2\text{Re}P_{1,2}, & \bar{Q}_{1,2} &= 2\text{Re}Q_{1,2}, \\ V &= 3|\Omega_1\Omega_2|^2(\bar{P}_1\bar{P}_2 - \bar{Q}_1\bar{Q}_2) + 2\gamma_2|\Omega_1|^2 \\ &\quad \times (\bar{P}_1 + \bar{Q}_1) + 2\gamma_1|\Omega_2|^2(\bar{P}_2 + \bar{Q}_2).\end{aligned}\quad (\text{A4})$$

### APPENDIX B: EFFECTIVE HAMILTONIAN

In this Appendix we derive the effective Hamiltonian from Eq. (11). We tune the cavity fields  $\delta_{1,2} = \pm\delta + \tilde{\delta}/2$ , and assume that  $(\Omega, \delta) \gg |\delta - \bar{\Omega}| \gg (\tilde{\delta}, |g_l\langle a_l \rangle|, \gamma_l, \kappa_l)$ ,  $l = 1, 2$ . In this case, the two-photon transitions are dominant over the one-photon transitions. The effective Hamiltonian can be derived by following the same techniques as in Ref. [32]. The equation for the density matrix is

$$\dot{\rho} = -\frac{i}{\hbar}[H'_I, \rho], \quad (\text{B1})$$

and we have its formal solution  $\rho(t) = \rho(0) - \frac{i}{\hbar} \int_0^t dt' [H'_I(t'), \rho(t')]$ . Substituting the solution back we obtain

$$\dot{\rho} = -\frac{i}{\hbar}[H'_I, \rho(0)] - \frac{i}{\hbar}\left[H'_I(t), -\frac{i}{\hbar} \int_0^t [H'_I(t'), \rho(t')]\right]. \quad (\text{B2})$$

For  $|\delta - \bar{\Omega}| \gg (|g_l\langle a_l \rangle|, \gamma_l)$  ( $l = 1, 2$ ) the first term is fast oscillating compared with the second one and is negligible to a good approximation. Then we can employ a Markovian approximation for the latter. In this approximation,  $H'_I$  in Eq. (B1) can be substituted for

$$H''_I = H'_I(t) \int H'_I(t') dt', \quad (\text{B3})$$

where the indefinite integral is evaluated at time  $t$  without integral constant. These arguments can be placed on a more rigorous footing by considering time-averaged dynamics over a period much longer than the period of any of the oscillations present in the effective Hamiltonian, i.e.,  $t \gg |\delta \pm \bar{\Omega}|^{-1}$ . Also, the secular approximation is made again. We can remove the dynamical stark shift and obtain the effective Hamiltonian

$$H''_I = H_1 + H_2 \quad (\text{B4})$$

with

$$\begin{aligned}H_1 &= \sum_{l=1,2} \hbar a_l^\dagger a_l [v_l(\sigma_{00} - \sigma_{++}) - \tilde{v}_l(\sigma_{00} - \sigma_{--})] \\ &\quad + \hbar[(v_2 - \tilde{v}_1)\sigma_{00} - v_1\sigma_{++} + \tilde{v}_2\sigma_{--}]\end{aligned}\quad (\text{B5})$$

and

$$\begin{aligned}H_2 &= \hbar(v^*a_1a_2 + va_1^\dagger a_2^\dagger)(\sigma_{00} - \sigma_{++}) \\ &\quad + \hbar(\tilde{v}^*a_1a_2 + \tilde{v}a_1^\dagger a_2^\dagger)(\sigma_{00} - \sigma_{--}),\end{aligned}\quad (\text{B6})$$

where we have used

$$\begin{aligned}v_1 &= \frac{G_1G_1^*}{\delta - \bar{\Omega}}, & \tilde{v}_1 &= \frac{\tilde{G}_1\tilde{G}_1^*}{\delta - \bar{\Omega}}, \\ v_2 &= \frac{G_2G_2^*}{\delta - \bar{\Omega}}, & \tilde{v}_2 &= \frac{\tilde{G}_2\tilde{G}_2^*}{\delta - \bar{\Omega}}, \\ v &= \frac{G_1^*G_2}{\delta - \bar{\Omega}}, & \tilde{v} &= \frac{\tilde{G}_1\tilde{G}_2^*}{\bar{\Omega} - \delta}.\end{aligned}\quad (\text{B7})$$

Close to the dark resonance ( $|\Delta| \ll \Omega$ ), all atoms are almost in the dark state  $\langle \sigma_{00} \rangle \approx 1$ . Under such conditions we make a unitary transformation with  $\exp(-iH_1t/\hbar)$ . Then, including the contribution of  $N$  atoms, taking  $\tilde{\delta} = \frac{(g_2^2 - g_1^2)N}{4(\sqrt{2}\Omega - \delta)}$  to remove the dynamic Stark shift of the atomic ensemble, we have the effective Hamiltonian (11) in the main text.

### APPENDIX C: THE OUTPUT FLUCTUATION SPECTRA

We present the calculation for the correlation spectra. In order to calculate quantum correlation spectra, we linearize Eqs. (14) around the semiclassical state corresponding to a stable working point. Writing  $\delta O(t) = O(t) - \langle O \rangle$ , we obtain the following equation written in a compact form, describing to first order the fluctuations in the field variables [27]:

$$\frac{d}{dt}\delta O(t) = -B\delta O(t) + F(t), \quad (\text{C1})$$

where  $\delta O = (\delta\alpha_1, \delta\alpha_2, \delta\alpha_1^*, \delta\alpha_2^*)$  and  $F(t) = (F_{\alpha_1}, F_{\alpha_2}, F_{\alpha_1^*}, F_{\alpha_2^*})^T$ . Using the Fourier transformation  $\delta O(\omega) = \frac{1}{\sqrt{2\pi}} \int_{-\infty}^{\infty} \delta O(t) e^{i\omega t} dt$ , the correlation spectrum is derived as [27]  $\langle \delta O(\omega) \delta O(\omega') \rangle = S(\omega) \delta(\omega + \omega')$ , where

$$S(\omega) = (B + i\omega I)^{-1} D (B^T - i\omega I)^{-1}, \quad (\text{C2})$$

where  $I$  is a unit matrix. The drift matrix  $B$  and the vector  $F(t)$  can be obtained from the set of Langevin equations (14). The spectrum exists if the steady-state solutions are stable. The stability can be verified by calculating the eigenvalues of the matrix  $B$ . When the real parts of all eigenvalues are positive, then the system is stable. The stability condition is derived as  $\xi < \sqrt{\kappa_1 \kappa_2}$ .

For the coherent inputs, by using the input-output relations [27]  $a_l^{\text{in}} + a_l^{\text{out}} = \sqrt{2\kappa_l} a_l$  ( $l = 1, 2$ ), we derive the output

fluctuation spectra in Eq. (17) as

$$\begin{aligned} S_{X_2}^{\text{out}}(\omega) &= 1 + 2\text{Re}[\kappa_1(S_{11} + S_{13}) + \kappa_2(S_{22} + S_{24}) \\ &\quad + 2\sqrt{\kappa_1 \kappa_2}(S_{12} + S_{23})], \\ S_{P_2}^{\text{out}}(\omega) &= 1 + 2\text{Re}[\kappa_1(S_{13} - S_{11}) + \kappa_2(S_{24} - S_{22}) \\ &\quad - 2\sqrt{\kappa_1 \kappa_2}(S_{12} - S_{23})]. \end{aligned} \quad (\text{C3})$$

The spectra at zero frequency ( $\omega = 0$ ) are reduced to Eqs. (18) in the main text.

- 
- [1] M. O. Scully and M. S. Zubairy, *Quantum Optics* (Cambridge University Press, Cambridge, 1997).
  - [2] D. F. Walls and G. J. Milburn, *Quantum Optics* (Springer, Berlin, 1994).
  - [3] R. W. Boyd, *Nonlinear Optics*, 3rd ed. (Academic, New York, 2008).
  - [4] A. Einstein, B. Podolsky, and N. Rosen, Can quantum-mechanical description of physical reality be considered complete? *Phys. Rev.* **47**, 777 (1935).
  - [5] S. L. Braunstein and P. van Loock, Quantum information with continuous variables, *Rev. Mod. Phys.* **77**, 513 (2005).
  - [6] M. D. Reid, D. F. Walls, and B. J. Dalton, Squeezing of Quantum Fluctuations via Atomic Coherence Effects, *Phys. Rev. Lett.* **55**, 1288 (1985).
  - [7] R. Guzmán, J. C. Retamal, E. Solano, and N. Zagury, Field Squeeze Operators in Optical Cavities with Atomic Ensembles, *Phys. Rev. Lett.* **96**, 010502 (2006).
  - [8] X. Liang, X. M. Hu, and C. He, Creating multimode squeezed states and Greenberger-Horne-Zeilinger entangled states using atomic coherent effects, *Phys. Rev. A* **85**, 032329 (2012).
  - [9] X. M. Hu and X. Li, Quantum interference in enhanced parametric interactions, *J. Phys. B* **43**, 055502 (2010); X. Li and X. M. Hu, Quantum beats and wave mixing interactions in Raman systems: Multimode squeezed and entangled states, *Laser Phys. Lett.* **10**, 075202 (2013).
  - [10] E. Arimondo, Coherent population trapping in laser spectroscopy, in *Progress in Optics*, Vol. 35, edited by E. Wolf (Elsevier Science, Amsterdam, 1996), p. 257.
  - [11] S. E. Harris, Electromagnetically induced transparency, *Phys. Today* **50**(7), 36 (1997).
  - [12] J. P. Marangos, Electromagnetically induced transparency, *J. Mod. Opt.* **45**, 471 (1998).
  - [13] M. D. Lukin, Trapping and manipulating photon states in atomic ensembles, *Rev. Mod. Phys.* **75**, 457 (2003).
  - [14] M. Fleischhauer, A. Imamoglu, and J. P. Marangos, Electromagnetically induced transparency: Optics in coherent media, *Rev. Mod. Phys.* **77**, 633 (2005).
  - [15] H. Schmidt and A. Imamoglu, Giant Kerr nonlinearities obtained by electromagnetically induced transparency, *Opt. Lett.* **21**, 1936 (1996).
  - [16] M. D. Lukin, A. B. Matsko, M. Fleischhauer, and M. O. Scully, Quantum Noise and Correlations in Resonantly Enhanced Wave Mixing Based on Atomic Coherence, *Phys. Rev. Lett.* **82**, 1847 (1999).
  - [17] A. André, L. M. Duan, and M. D. Lukin, Coherent Atom Interactions Mediated by Dark-State Polaritons, *Phys. Rev. Lett.* **88**, 243602 (2002).
  - [18] Y. P. Niu, S. Q. Gong, R. X. Li, Z. Z. Xu, and X. Y. Liang, Giant Kerr nonlinearity induced by interacting dark resonances, *Opt. Lett.* **30**, 3371 (2005).
  - [19] J. Kou, R. G. Wan, Z. H. Kang, H. H. Wang, L. Jiang, X. J. Zhang, Y. Jiang, and J. Y. Gao, EIT-assisted large cross-Kerr nonlinearity in a four-level inverted-Y atomic system, *J. Opt. Soc. Am. B* **27**, 2035 (2010).
  - [20] C. Hang and G. X. Huang, Giant Kerr nonlinearity and weak-light superluminal optical solitons in a four-state atomic system with gain doublet, *Opt. Express* **18**, 2952 (2010).
  - [21] H. Wang, D. Goorskey, and M. Xiao, Enhanced Kerr Nonlinearity via Atomic Coherence in a Three-Level Atomic System, *Phys. Rev. Lett.* **87**, 073601 (2001); Dependence of enhanced Kerr nonlinearity on coupling power in a three-level atomic system, *Opt. Lett.* **27**, 258 (2002).
  - [22] A. Dantan, J. Cviklinski, E. Giacobino, and M. Pinard, Spin Squeezing and Light Entanglement in Coherent Population Trapping, *Phys. Rev. Lett.* **97**, 023605 (2006).
  - [23] A. Sinatra, Quantum Correlations of Two Optical Fields Close to Electromagnetically Induced Transparency, *Phys. Rev. Lett.* **97**, 253601 (2006).
  - [24] P. Barberis-Blostein and M. Bionert, Opacity of Electromagnetically Induced Transparency for Quantum Fluctuations, *Phys. Rev. Lett.* **98**, 033602 (2007).
  - [25] X. M. Hu, Entanglement generation by dissipation in or beyond dark resonances, *Phys. Rev. A* **92**, 022329 (2015); L. C. Li, X. M. Hu, S. Rao, and J. Xu, Noise squeezing of fields that bichromatically excite atoms in a cavity, *Opt. Express* **24**, 26536 (2016).
  - [26] C. Cohen-Tannoudji, J. Dupont-Roc, and G. Grynberg, *Atom-photon Interactions* (Wiley, New York, 1992).
  - [27] C. W. Gardiner and P. Zoller, *Quantum Noise*, 2nd ed. (Springer, Berlin, 2000).
  - [28] L. M. Duan, G. Giedke, J. I. Cirac, and P. Zoller, Inseparability Criterion for Continuous Variable Systems, *Phys. Rev. Lett.* **84**, 2722 (2000).
  - [29] R. E. S. Polkinghorne and T. C. Ralph, Continuous Variable Entanglement Swapping, *Phys. Rev. Lett.* **83**, 2095 (1999).
  - [30] X. J. Jia, X. L. Su, Q. Pan, J. R. Gao, C. D. Xie, and K. C. Peng, Experimental Demonstration of Unconditional Entanglement Swapping for Continuous Variables, *Phys. Rev. Lett.* **93**, 250503 (2004).
  - [31] M. Hennrich, T. Legero, A. Kuhn, and G. Rempe, Vacuum-Stimulated Raman Scattering Based on Adiabatic Passage in a High-Finesse Optical Cavity, *Phys. Rev. Lett.* **85**, 4872 (2000).
  - [32] D. F. V. James, Quantum computation with hot and cold ions: An assessment of proposed schemes, *Fortschr. Phys.* **48**, 823 (2000).